Aerodynamic Canard/Wing Parametric Analysis for General-Aviation Applications

Michael W. Keith* and Bruce P. Selberg†
University of Missouri, Rolla, Missouri

Vortex panel and vortex lattice methods have been utilized in an analytic study to determine the two- and three-dimensional aerodynamic behavior of canard/wing configurations. The purpose was to generate data useful for the design of general-aviation canard aircraft. Moderate two-dimensional coupling was encountered and the vertical distance between the lifting surfaces was found to be the main contributor to interference effects of the three-dimensional analysis. All canard configurations were less efficient than a forward wing with an aft horizontal tail, but were less sensitive to off-optimum division of total lift between the two surfaces, such that trim drag could be less for canard configurations. For designing a general-aviation canard aircraft, results point toward large horizontal and vertical distances between the canard and wing, a large wing-to-canard area ratio, and the canard at a low-incidence angle relative to the wing.

Nomenclature

AR	= aspect ratio
C_d	= sectional drag coefficient
C_D	= total drag coefficient
C_{Di}	= induced drag coefficient
$C_{d_{\min}}$	= minimum drag coefficient
C_ℓ	= sectional lift coefficient
C_{ℓ_0}	= sectional zero lift coefficient
C_{ℓ_α}	= sectional lift curve slope
C_L	= total lift coefficient
C_{L_α}	= total lift curve slope
c	= chord
D	= decalage angle
e	= span efficiency factor
G	= gap (in chord lengths)
L_{c_0}	= canard zero lift
L/D	= total lift-to-drag ratio
R_c	= Reynolds number based on chord
R_e	= Reynolds number per unit length
S	= stagger (in chord lengths)
S_C	= canard area
S_H	= horizontal tail area
S_W	= wing area
S_{ref}	= total reference area
λ	= taper ratio

Subscripts

C	= canard
H	= horizontal tail
W	= wing

Introduction

ALTHOUGH the first powered aircraft was a canard configuration, few successful canard aircraft are flying today. This has resulted from the misconception that canard aircraft are longitudinally unstable, an outgrowth of experience with the Wright flyer. Recently, canards have been applied to high-speed designs, but very little has been applied to transport or light aircraft. Rutan[1,2] has probably been the most notable and successful with canard configurations. He has clearly demonstrated, with his home-built "sports aircraft," that canard-configured aircraft can be longitudinally stable.

Canard aircraft are attractive because of the possibility of achieving stall-proof aircraft that may also have less drag and, hence, be more efficient. Typically, most conventional tail-aft aircraft fly with a download on the tail, a penalty suffered in order to trim the aircraft. The use of a canard should relieve the problem because canard aircraft trim with an upload on the canard. Thus, this should increase the overall efficiency of the aircraft by reducing the wing lift as well as the trim load normally associated with the downloading tail.

The terms associated with canard configurations are gap, stagger, and decalage. Gap is the vertical distance between the canard and wing and is always considered positive. Stagger is the horizontal distance between the canard and wing with positive stagger occurring when the canard, which is always forward of the wing, is above the wing. Decalage is the relative angle of incidence between the canard and wing, positive when the canard is at a higher angle of incidence than the wing. Both stagger and gap are measured from midchord to midchord and nondimensionalized with respect to the average chord length of the wing and canard. The dividing line between canard and tandem wing configurations is somewhat arbitrary and not really important here. For this investigation, it is assumed that a canard configuration is one in which the forward surface area is equal to or less than the rear surface area. Also, any configuration with small stagger, less than two average chord lengths, is considered to be a dual-wing configuration.

Even with the few successful canard aircraft flying, little quantitative data are available in the literature to design successful general-aviation canard aircraft. The material available has relied on the Prandtl-Munk theory or the equivalent lifting-line theory to measure the induced drag. It is the purpose of this paper to consider and discuss the interference effects and determine the "best" aerodynamic location and relative size of a canard wing using vortex panel analysis along with vortex lattice methods.

Canard/Wing Tradeoff Studies

Since most canard configuration work has been applied only to low aspect ratio swept wings of fighter and SST air-

Received April 15, 1984; revision received Dec. 18, 1984. Copyright © American Institute of Aeronautics and Astronautics, Inc., 1985. All rights reserved.

*Graduate Student, Mechanical and Aerospace Engineering Department; currently, Engineer, Gates Learjet, Wichita, Kansas. Member AIAA.

†Professor of Aerospace Engineering, Mechanical and Aerospace Engineering Department. Associate Fellow AIAA.

craft, it was necessary to study in detail all parameters and their effects on each other for high aspect ratio wings as applied to general-aviation aircraft. The aerodynamic effects of stagger S, gap G, decalage angle D, wing-to-canard area ratio S_W/S_C, aspect ratio $\mathcal{R}$, taper ratio λ, and winglets were determined by investigating the two-dimensional drag combined with the three-dimensional induced drag for different parameter combinations. These were investigated on a new medium-speed general-aviation airfoil, NASA MS(1)-0313.

The aerodynamic investigation was completed using an inviscid vortex panel multielement program coupled to a momentum integral boundary-layer analysis program. These predicted theoretical two-dimensional inviscid and viscid data. The results of the two-dimensional vortex panel analysis were used as input to a three-dimensional vortex lattice program to predict the induced drag of the finite lifting surfaces.

The laminar flow portion of the momentum integral program predicts the behavior of the boundary layer with Thwaites' method[3] and uses Michel's transition criterion[4] for smooth airfoils to determine the point of laminar-turbulent transition. The turbulent flow solution is obtained using Head's momentum integral method[5] with the two-dimensional drag calculated using the Squire-Young formula.[6] To determine the validity of the predicted two-dimensional drag, the analytical results were compared to experimental results[7,8] known at the same Reynolds number for smooth airfoils. Figure 1 compares the theoretical and experimental data for the MS(1)-0313 airfoil at a Reynolds number, R_c, of 4×10^6. The maximum deviation between experiment and theory is 12%. The analytical results used a Young's factor of 2.4 in the Squire-Young equation. The same good agreement was obtained for the airfoil at other Reynolds numbers.

The vortex lattice program used on this study was developed at the University of Missouri-Rolla (UMR). The vortex lattice induced drag combined with the viscous drag is compared in Fig. 2 with experimental NASA data after Paulson[9] formed a fuselage wing combination using a GAW-1 airfoil with an aspect ratio of 8.9.

There are few published reports that deal with canard or tandem wing configurations,[10-15] and most of these deal with the comparison of induced drag characteristics between canard and tail-aft aircraft and have relied on the Prandtl-Munk theory. But from the wind tunnel tests that were completed at Vought, Wolkovitch[10] pointed out that the analysis of separate component data showed that the measured two-dimensional drag coefficient, C_d, for the long coupled tandem wing configuration agreed closely with the sum of the C_d for each component. This indicates that the interference effects on two-dimensional drag are small. Figure 3 shows the calculated two-dimensional aerodynamic coupling between two MS(1)-0313 airfoils, as denoted by the ratio of the sectional canard-to-wing lift curve slopes, $C_{\ell_{\alpha C}}/C_{\ell_{\alpha W}}$.

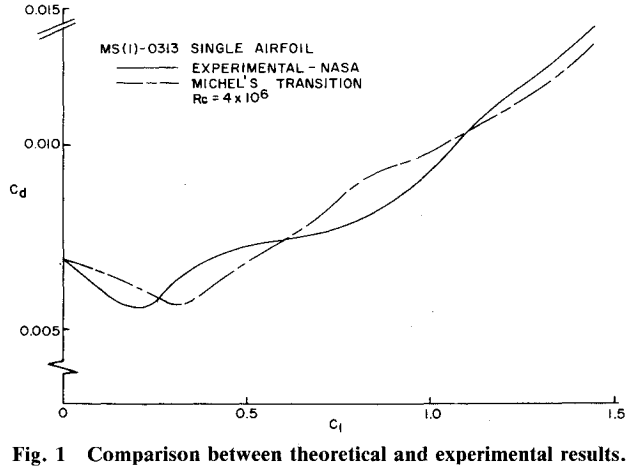

Fig. 1 Comparison between theoretical and experimental results.

Strong two-dimensional coupling occurs with a gap less than one and stagger less than three with moderate coupling for staggers between three and ten. These data represent all decalage angles considered. The surface pressure distributions were considered for the two-dimensional uncoupled cases for the canard and wing and were found to be identical to those of a wing alone in the freestream at the same lift coefficient, C_ℓ.

Even though the decalage angle has no two-dimensional aerodynamic effect on highly staggered configurations, there is an increase in two-dimensional drag for increases in absolute value of decalage angle. This results from the summation of the canard and wing component drag polars being essentially "out of phase" from each other. This is illustrated in Fig. 4, which shows the two-dimensional drag polar for the canard, wing, and total of the canard and wing at a configuration decalage angle of 2 deg. Both the wing and canard have equal chord lengths of 2.04 ft, which is used as the reference length in both cases. The reference chord of the total curve is the summation of the two individual chords. The decalage angle of 2 deg causes the canard and wing drag polars to be shifted horizontally away from each other such that each wing has a minimum drag coefficient $C_{d_{\min}}$ that corresponds to two different total lift coefficients C_ℓ, and the minimum total drag coefficient corresponds to yet another C_ℓ which is between the respective C_ℓ value for $C_{d_{\min}}$ for each wing and canard. Conse-

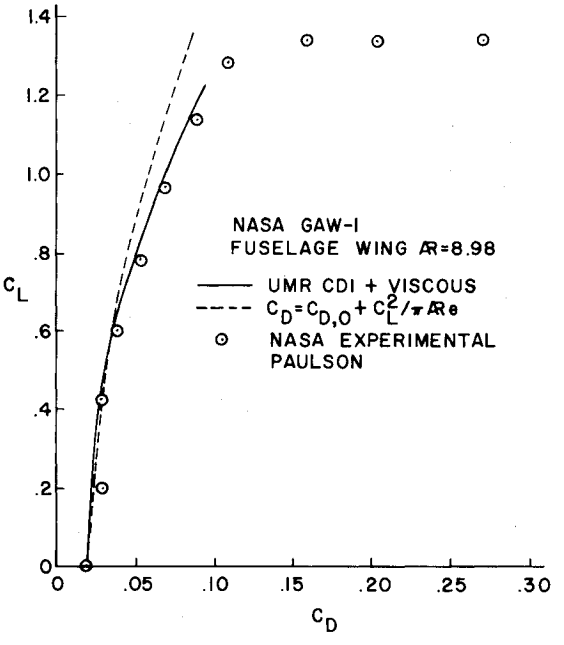

Fig. 2 Vortex lattice program and viscous drag comparison.

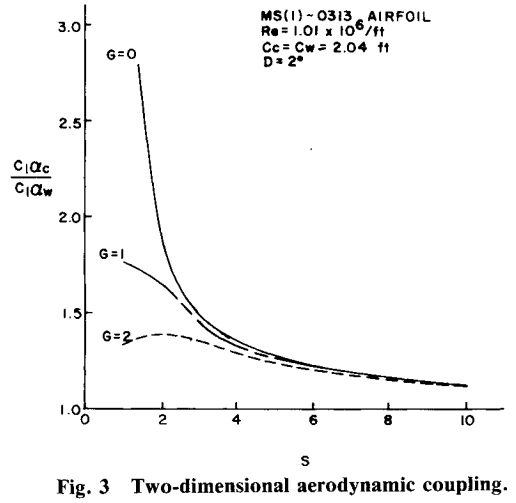

Fig. 3 Two-dimensional aerodynamic coupling.

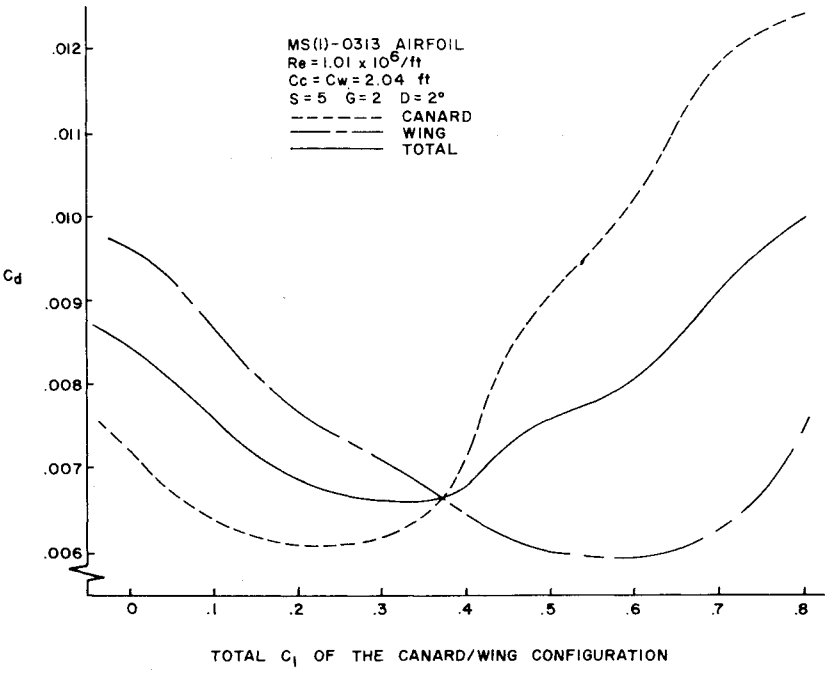

Fig. 4 Two-dimensional drag polar for the canard, wing, and total of the canard and wing.

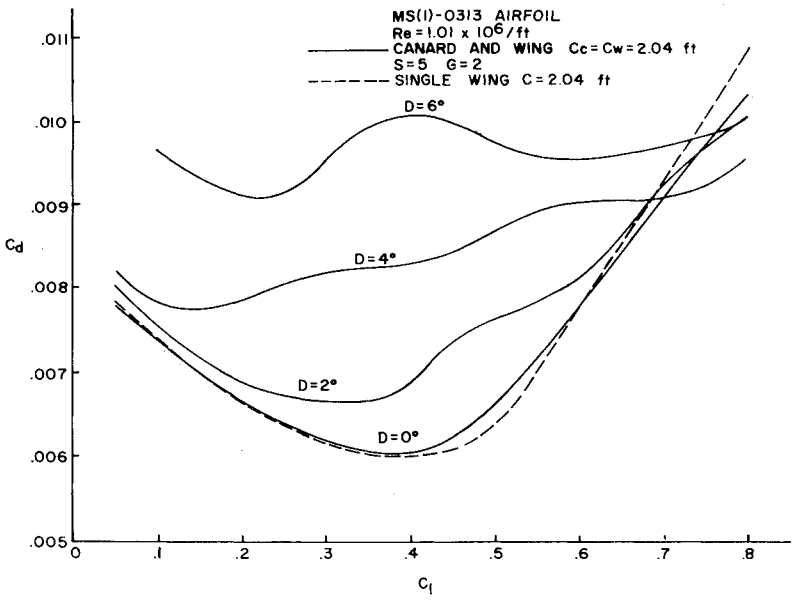

Fig. 5 Two-dimensional drag polar comparison between several decalage angles and a single wing.

quently, the overall drag polar is shifted upward and there is an increase in two-dimensional drag at a given C_ℓ. There is also a slight increase in two-dimensional drag over that of a single wing at $D=0$ deg because of the difference in the two-dimensional lift curve slope C_{ℓ_α}, and the zero lift coefficient C_{ℓ_0}, of the two lifting surfaces. In order to achieve trim, typical canard configurations need a positive decalage which increases the two-dimensional drag. Figure 5 shows the effects of increasing positive decalage angle and also compares the single wing drag polar at the same reference chord length.

Complementing two-dimensional aerodynamic coupling, the remainder of this section discusses the induced drag levels of various combinations of the two lifting surfaces. Wolkovitch,[10] Tulinius and Margason,[11] Feistel et al.,[12] and McLaughlin[14] all agree, from Prandtl-Munk's theorem, that there is a considerable induced drag savings for configurations with large gap as measured in the Trefftz plane. From their powered canard/wing research configuration, with relatively low aspect ratio swept wings, and largest possible gap, Tulinius and Margason[11] noted as much as a 28% increase in the span efficiency factor e over the canard/wing, where the canard was in the same plane as the wing. Efficiency, as predicted by the vortex lattice program, of a canard/wing combination with $G=4$ is 40% greater than with $G=0$. However, by placing a typical fuselage height constraint on the gap such that the gap is no more than 2 or 3 still yields results of about a 25 or 30% increase in e over the zero gap combination. This is in excellent agreement with Tulinius and Margason[11] although this study is for high aspect ratio straight wings. The span efficiency factor was predicted for a very broad range of lift coefficient, $0.3 < C_L < 1.0$, and for all highly staggered configurations, $|S| > 2$. For stagger less than 2, the trends are the same except there are greater losses in e at lower gaps. Three-dimensional effects of stagger for several C_L values were determined, but the results of varying stagger did not indicate an advantage of positive stagger (canard above the wing) over negative stagger (canard below the wing) as Feistel et al.[12] noted for very small stagger, $S=1.63$, with rectangular planforms and aspect ratios equal to 6. Their conclusion was that the low canard tip vortices caused unfavorable interference on the wing lift by passing under instead of over the wing for the high canard configuration. But

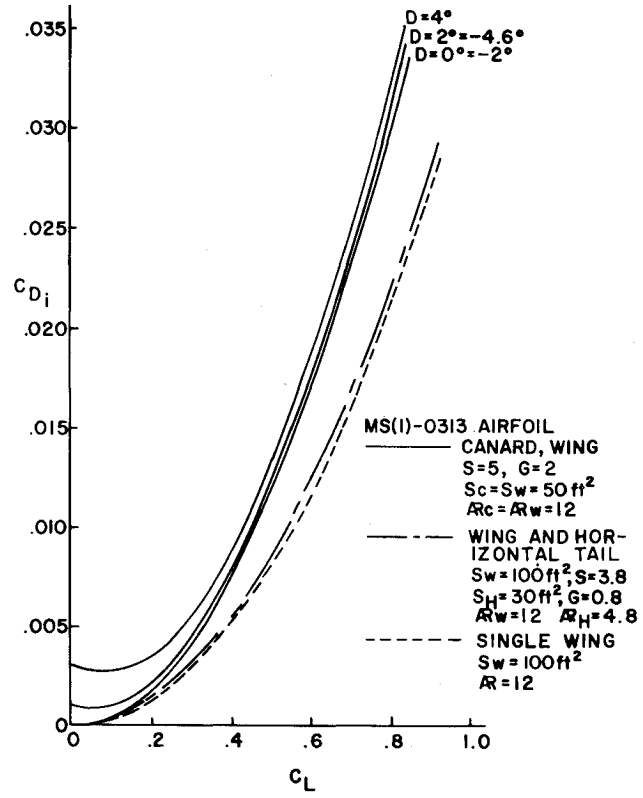

Fig. 6 Induced drag polar comparison between canard and tail-aft configurations and a single wing.

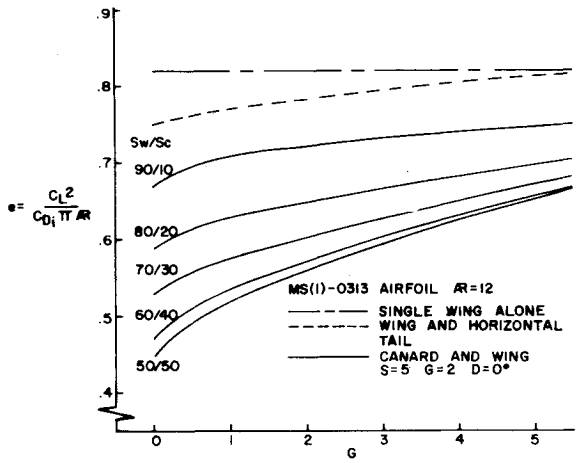

Fig. 7 Span efficiency factor comparison between different wing-to-canard area ratios.

even their results were not as noticeable at high stagger (which incidentally corresponds to $S=3$ herein), and they concluded that the wing and canard act more like two independent surfaces at high stagger. The UMR vortex lattice program accounts for upwash and downwash outboard of a particular surface. However, it does not account for the trailing tip vortices and thus is unable to show the induced drag advantage of low canard (positive stagger) configurations.

Investigating the wing/canard combinations in more detail quickly showed a considerable amount of induced three-dimensional coupling between the two lifting surfaces even at highly staggered and gapped configurations ($S \geq 5$ and $G \geq 2$). Both the canard and wing have an increase in induced drag as compared to a single wing alone. It is evident that the canard is affected by the upwash of the wing, and the wing is degraded considerably by the downwash of the canard. The interference

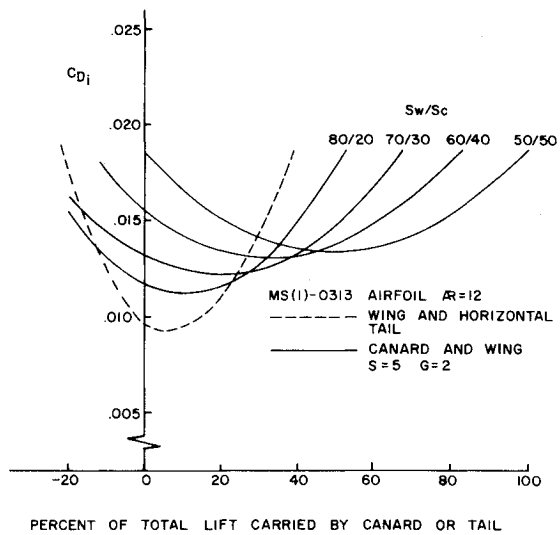

Fig. 8 Trim drag sensitivity to total lift distribution between the canard and wing.

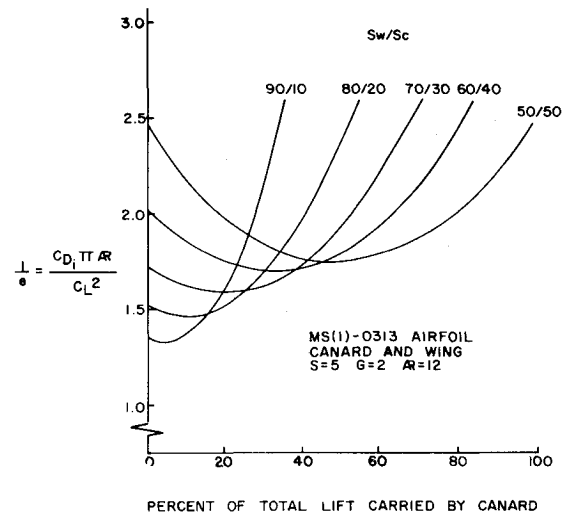

Fig. 9 Span efficiency reciprocal factor for different wing-to-canard area ratios.

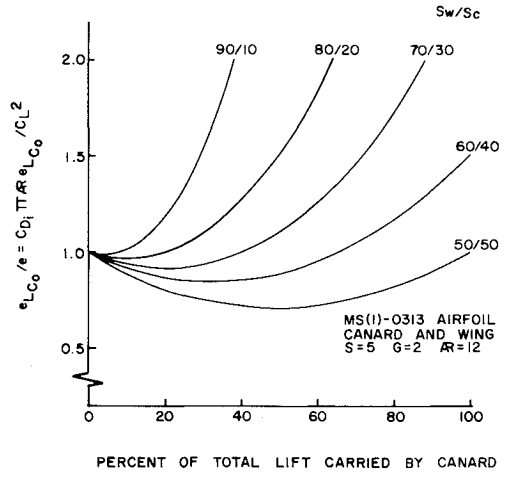

Fig. 10 Span efficiency reciprocal factor normalized to canard zero lift.

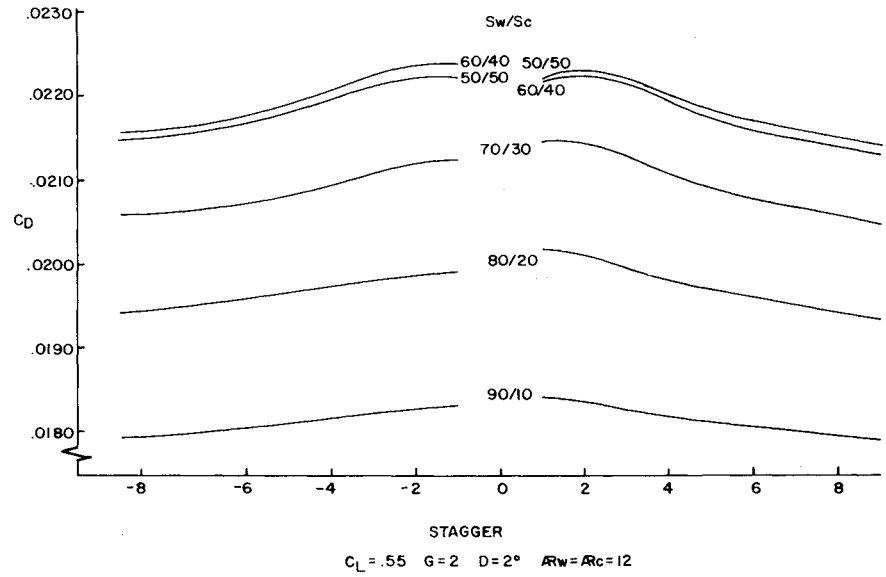

Fig. 11 Effect of total wing drag and area ratios.

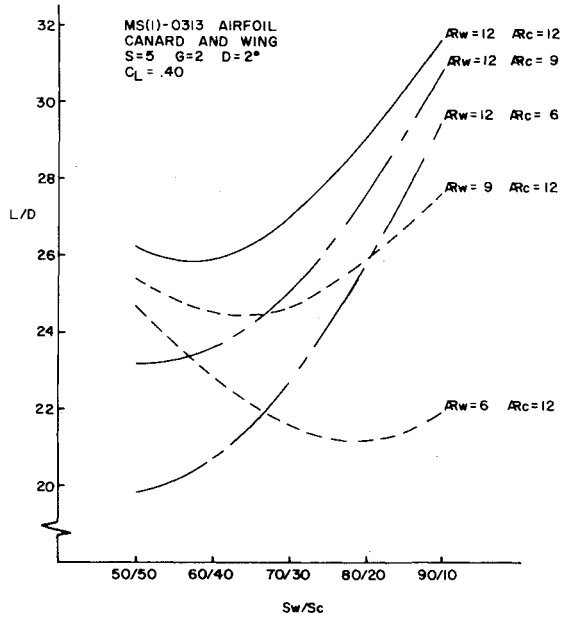

Fig. 12 Lift-to-drag ratio effects with different combinations of wing and canard aspect ratios.

does not occur only for a tandem-canard/wing configuration, but whenever an additional wing surface is added to the freestream, such as is the case with all conventional aircraft that have an aft-horizontal tail. Figure 6 shows the comparison of the total induced drag polars of the canard/wing configuration at several values of decalage, the total induced drag polar of the wing/tail configuration, and the single wing in the freestream with no extra horizontal surface affecting its flowfield. This shows the unfortunate penalty of adding an additional lifting surface to the freestream, and the amount the tail interference degrades the performance of just a single wing. Equally important, Fig. 6 shows the increase in induced drag with increase in decalage angle for the canard/wing configuration. Note the substantial increase in induced drag at low C_L values at $D=4$ deg, as compared to $D=0$ deg. This increase in induced drag at low C_L values is very similar to that of the two-dimensional drag polars, where the wing and canard drag polars are essentially "out of phase" from each other. Just as for the two-dimensional drag polars, an increase in absolute value of decalage angle will tend to shift the curves vertically upward, thereby increasing the induced drag levels at all C_L values. Because of the difference in total wing and canard lift curve slopes, $C_{L_{\alpha W}}$ and $C_{l_{\alpha C}}$, $D=0$ deg is not the minimum induced drag level, but rather closer to $D=-2$ deg. The total induced drag is the least at $D=-2$ deg because the canard and wing drag polars "match up" and are equal.

Thus far the three-dimensional induced drag results have pointed toward a savings when the canard configuration has large gap and a decalage angle equal to -2 deg. Stagger varied the induced drag only slightly. However, it is equally important to consider different wing-to-canard area ratios, S_W/S_C. This was done by keeping total lifting area the same ($S_{\text{ref}} = 100$ ft^2), and the aspect ratio of each individual lifting surface constant ($\mathcal{R}_W = \mathcal{R}_C = 12$). The wing-to-canard area ratios investigated included $S_W/S_C = 50/50$, 60/40, 70/30, 80/20, and 90/10.

It was necessary to consider a broad range of area ratios because a quick stability analysis of canard configurations demonstrated that stability can be attained at any wing-to-canard area ratio. This is in agreement with Ref. 11.

The work up to this point only involved the tandem wing configuration, an area ratio of $S_W/S_C = 50/50$. Figure 7 shows the increase in e with increase in wing-to-canard area ratio. At small gap values, the large area ratio has a value of e 45% percent higher than the ratio for equal lifting areas. This figure shows that the configurations with a less percentage of canard lifting area are not degraded by gap nearly as much as the more tandem configurations. As the wing-to-canard area ratio increases, e also increases, stays more constant with gap, and approaches that of the single wing. Figure 7 also shows the relationship of the wing/tail combination.

Although the induced drag is more for the canard configuration, Fig. 8 illustrates why the canard configuration should not be dismissed when compared to the tail-aft configuration. Although Fig. 8 shows that the minimum induced drag is less for the conventional tail-aft configuration, more importantly, it shows that the excess above minimum (i.e., the trim drag) is less sensitive to off-optimum division of total lift between the two lifting surfaces for the more tandem wing configuration. This means the canard configuration can be off-loaded much more drastically to obtain trim static longitudinal stability and not be penalized nearly as much as the conventional tail aft would be. This sensitivity of off-loading of the canard configuration was also recognized by Wolkovitch.[10]

McLaughlin[13] also compares the induced drag coefficients of conventional and canard configurations, but uses the classical minimum-drag theory. He shows that a canard con-

figurations has greater induced drag and that the induced drag coefficient decreases for both conventional and canard configuration as gap increases. But he also finds that a tandem configuration ($S_W/S_C = 50/50$) has the lowest induced drag, which is in direct disagreement with the results plotted in Figs. 7 and 8. Feistel et al.,[13] who use the classical Prandtl-Munk expression, also agree with McLaughlin.[13] In order to show the analysis in a different way, a graph similar to that of Fig. 8 was constructed. Figure 9 shows the reciprocal of span efficiency factor, $1/e$, as a function of the percent of the total lift carried by the canard. Since it is desirable to have the span efficiency factor high, then the reciprocal should be low. Figure 9 shows that $1/e$ is lowest for the largest wing-to-canard area ratio ($S_W/S_C = 90/10$) and highest for the tandem wing configuration ($S_W/S_C = 50/50$). Once again, this shows that the largest wing-to-canard area ratio is the most efficient in terms of three-dimensional induced drag.

Figure 10 is obtained by dividing each of the wing-to-canard area ratio curves of Fig. 9 by the individual span efficiency factor, $e_{L_{CO}}$, i.e., that which is obtained at canard zero lift, L_{CO}. This figure is identical to those presented by Feistel et al.,[13] where the induced drag parameter $1/e$ was calculated from the Prandtl-Munk theory. Referring only to this figure, one would conclude that the most efficient case is the area ratio of $S_W/S_C = 50/50$. This suggests that the results obtained from using the Prandtl-Munk expression may be misinterpreted because of the offset in the induced drag polars (and, therefore, the reciprocal efficiency polars) of the canard configuration. The offset in the drag polar or reciprocal efficiency polar is produced by the minimum drag not occurring at a canard lift of zero, but rather at some higher percentage (up to 50%) of the total lift. Wolkovitch[10] mentions that several problems arise in comparing experimental drag data with the predictions given by the Prandtl-Munk expression because the Prandtl-Munk expression does not account for the offset in the induced drag.

The total wing drag coefficient, as a function of stagger and wing-to-canard area ratio, is shown in Fig. 11 for a typical cruise lift coefficient of 0.55 at $G = 2$ and $D = 2$ deg. Due to the two- and three-dimensional interaction, the drag coefficient increases as the canard gets larger and, hence, produces more canard-to-wing flow interaction. The drag coefficient also increases as the absolute value of stagger decreases, again due to the stronger flow coupling. Note that these results will differ from a conventional wing/horizontal tail arrangement in that the decalage angle will be negative for the conventional wing/tail configuration implying lower two-dimensional position of the drag, as shown in Fig. 5.

One additional parameter was considered in the three-dimensional tradeoff analysis. This was the aspect ratio variance between the two lifting surfaces. The canard and wing aspect ratio values were both varied individually between 6 and 12. It was determined that the highest aspect ratio for both lifting surfaces was the most efficient for all wing-to-canard area ratios. A decrease in either wing or canard aspect ratio or both causes an increase in induced drag at all values of C_L. More pronounced effects of decreasing performance were obtained at higher values of C_L as compared to the lower C_L values. Figure 12 shows the effects of aspect ratio by illustrating the total lift to drag relationship L/D for the canard/wing combination at a particular lift coefficient, $C_L = 0.4$, for all values of wing-to-canard area ratio. This figure combines the two-dimensional drag and the three-dimensional induced drag, and clearly shows that the higher the aspect ratio, the better the aerodynamic performance. Again, this figure is very representative of all C_L values considered. Notice that as $\mathcal{R}_C$ decreases from 12 to 6, L/D decreases approximately 25% at $S_W/S_C = 50/50$ and approximately only 7% at $S_W/S_C = 90/10$. This is explained by the fact that the canard carries a higher percentage of the lift at a smaller area ratio than at a larger area ratio. Just the opposite is the case as $\mathcal{R}_W$ decreases from 12 to 6, L/D decreases approximately 31% as $S_W/S_C = 90/10$ and approximately only 6% at $S_W/S_C = 50/50$. Again the same reasoning stands, but the wing carries a higher percentage of the load at the larger area ratio and, therefore, the configurations with larger values of area ratio are affected more by the decreasing wing aspect ratio.

Figures 13 and 14 illustrate the overall trends of two- and three-dimensional lifting surface drag. Neither curve considers the interaction between the viscous and induced drag. However, at $C_L = 0.55$ the induced angles of attack will not change the viscous drag significantly and the results shown in Figs. 13 and 14 are representative of actual stagger and

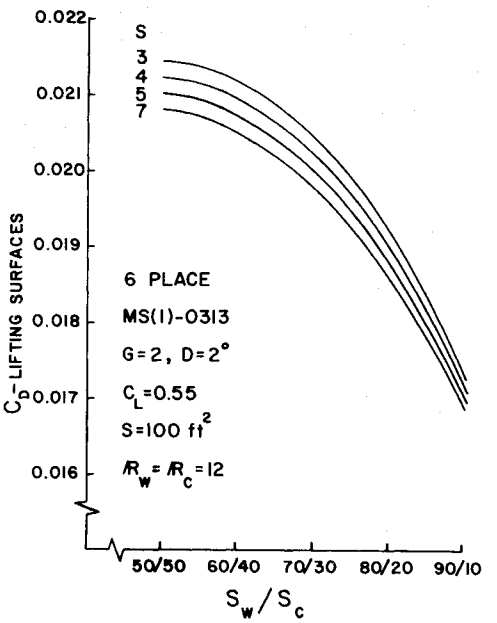

Fig. 13 Total drag coefficient for variation of stagger and wing-to-canard area ratios.

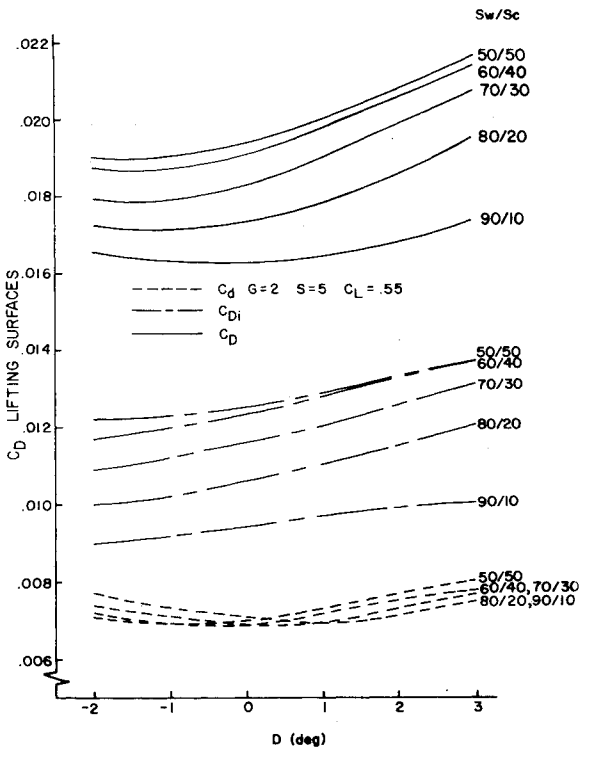

Fig. 14 Two- and three-dimensional drag coefficient breakdown for decalage angle variations.

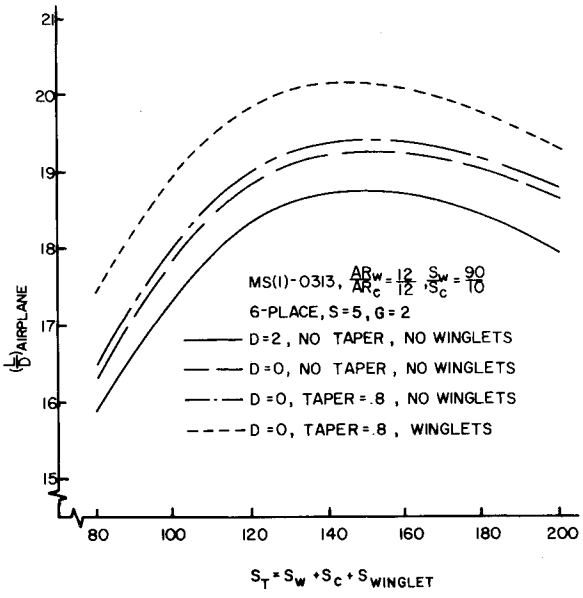

Fig. 15 Total airplane effects of decalage, taper ratio, and winglets.

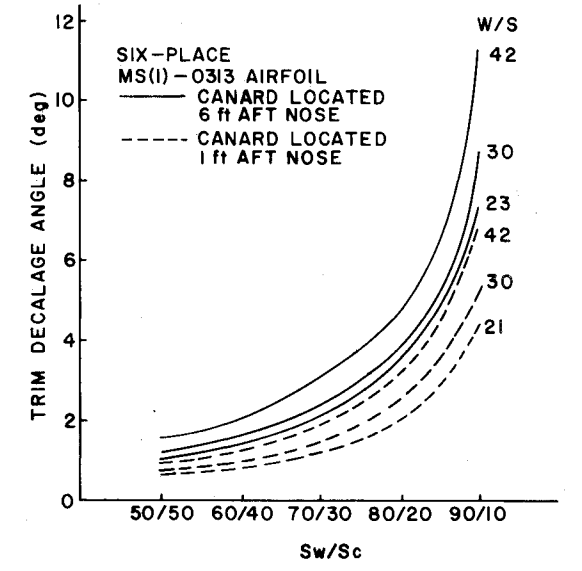

Fig. 16 Airplane trim decalage with area ratio.

decalage results for various wing-to-canard area ratios. Figure 13 shows the total drag coefficient, $C_{DLS}=C_d+C_{Di}$, of the lifting surfaces for increasing wing-to-canard area ratio for various stagger values. It shows an approximate 16% decrease in drag for an increase in area ratio from $S_W/S_C=50/50$ to 90/10 at $C_L=0.55$. Note also that as S_W/S_C increases, the canard configurations become less sensitive to stagger. Figure 14 shows the two- and three-dimensional lifting surface drag coefficients, C_d and C_{Di}, as well as the total drag coefficient, C_{DLS}, as a function of decalage angle for the area ratios considered at $C_L=0.55$. It shows that the three-dimensional effects are more pronounced and more sensitive to area ratio and decalage angle than the two-dimensional effects. The two-dimensional minimum drag occurs at approximately $D=0$ deg, whereas the three-dimensional minimum drag occurs at $D=-2$ deg. It illustrates that the largest area ratio has the least total drag and that a decalage angle between -2 and -1 deg is the minimum total drag angle for all area ratios. Again, these figures are very representative of the drag trends at all C_L values, however, the optimum C_L would be lower, i.e., a C_L such that the two- and three-dimensional drag coefficients would be equal. It should be pointed out that not all of the configurations shown in Figs. 13 and 14 are stable. However, recent work on three surface configurations by Kendall[16] and Rokhsaz and Selberg[17] have shown reduced induced drag for trisurface configurations. The application to this work is the potential of being able to trim the higher wing-to-canard area ratios with a third surface, thereby lowering the trim drag penalty.

Winglets were analyzed thoroughly with the vortex lattice program to determine the best angle of incidence, sweep, and other dimensions. That analysis and detail have not been included here, but the effect of winglets and taper ratio are shown in Fig. 15 for a typical general-aviation configuration as a function of total lifting area. The combination of winglets and taper has a significant effect at all area ratios.

All of the above analyses ignored trim effects. Figure 16 shows the trim decalage angle for a typical general-aviation configuration as a function of wing-to-canard area ratio and total wing and canard loading. Static margins for this typical case varied from -0.1 for the aft center of gravity to -1.6 for the forward location of the center of gravity. As the decalage angle increases the canard loading increases, hence increasing the wing loading. Here the highest wing-to-canard area ratios require the largest trim decalage angle and, hence a higher trim drag penalty.

Concluding Remarks

Vortex panel and vortex lattice methods have been utilized to determine the aerodynamic effects of stagger, gap, decalage, wing-to-canard area ratio, and aspect ratio as applied to canard/wing configurations. Strong two-dimensional coupling was found to occur with gap less than one and stagger less than three, otherwise the two surfaces were moderately coupled two dimensionally. However, because of a horizontal shift of the individual lifting surface drag polars at nonzero decalage angle, the two-dimensional drag polars shift upward causing an increase in drag due to decalage angle.

Gap is the main contributor to interference effects of induced drag, but some interference is encountered with different decalage angles, and very little for varying stagger values. As much as a 30% decrease in induced drag can be obtained if the two surfaces are out of plane and have nominal gaps. Untrimmed drag was found to decrease with increasing wing-to-canard area ratio. All canard configurations were less efficient than a forward wing with an aft horizontal tail, but the excess above minimum drag, i.e., trim drag, was less sensitive to off-optimum division of total lift between the two surfaces for canards as compared to the conventional tail-aft configuration, with equal areas being least sensitive. It was determined that the highest aspect ratio for both lifting surfaces was the most efficient for all wing-to-canard area ratios and the smaller the total load on the surface, the less sensitive that surface was to decreasing aspect ratio.

For the canard configurations considered, the three-dimensional effects were much greater than the two dimensional. Without considering any other design criteria for light aircraft except minimum drag, it would be best to design a canard aircraft that could have maximum stagger, gap, aspect ratio, and wing-to-canard area ratio with the lowest decalage angle that would allow trim flight.

Acknowledgment

The results presented herein were obtained from research funded by NASA Research Grant NAG1-26 administered by Langley Research Center under the direction of Dr. Bruce Holmes.

References

[1]Rutan, B., "Development of Small High-Aspect-Ratio Canard Aircraft," *Cockpit*, Vol. 13, No. 2, 1980, pp. 93-101.

[2]Rutan, B., "Tale of the Three EZ's," *Sport Aviation*, Vol. 29, No. 2, Feb. 1980, pp. 34-39.

[3]Thwaites, B., "Approximate Calculation of the Laminar Boundary Layer," *Aeronautical Quarterly I*, Vol. 1, 1949, pp. 245-283.

[4]Michel, R., "Etude de la Transition sur les Profiles d'Aile, Establissement d'un Critere de Determination de Point de Transition et Calcul de la Trainee de Profile Incompressible," ONERA Rept. 1/1578A, 1951.

[5]Cebeci, T. and Bradshaw, P., *Momentum Transfer in Boundary Layers*, Hemisphere Publishing Corp., Washington, D.C., 1977, pp. 192-194.

[6]Cebeci, T. and Smith, A. M. O., "Calculation of Profile Drag of Airfoils at Low Mach Numbers," *Journal of Aircraft,* Vol. 5, Nov.-Dec. 1968, pp. 535-542.

[7]McGhee, R. J., "Wind Tunnel Results for a 13-Percent-Thick Medium Speed Airfoil Section," NASA-TP-1498, 1981.

[8]Somers, D. M., "Design and Experimental Results for a Flapped Natural-Laminar-Flow Airfoil for General Aviation Applications," NASA TR-1865, June 1981.

[9]Paulson, J. W., "Application of Vortex Lattice Theory to Preliminary Aerodynamic Design," NASA TN-D-8236 NASA Langley Research Center, Langley Station, Va., 1976.

[10]Wolkovitch, J., "Subsonic VSTOL Aircraft Configurations with Tandem Wings," *Journal of Aircraft*, Vol. 16, Sept. 1979, pp. 605-611.

[11]Tulinius, J. R. and Margason, R. J., "Aircraft Aerodynamic Design and Evaluation Methods," AIAA Paper 76-15, 1976.

[12]Feistel, T. W., Corsiglia, V. R., and Levin, D. B., "Wind-Tunnel Measurements of Wing-Canard Interference and a Comparison with Various Theories," SAE Paper 810575, 1981.

[13]McLaughlin, M. D., "Calculations and Comparison with an Ideal Minimum of Trimmed Drag for Conventional and Canard Configurations Having Various Levels of Static Stability," NASA TN D-8391.

[14]Goldstein, S. E. and Combs, C. P., "Trimmed Drag and Maximum Flight Efficiency of Aft Tail and Canard Configurations," AIAA Paper 74-69, 1974.

[15]Laitone, E. V., "Prandtl's Biplane Theory Applied to Canard and Tandem Aircraft," *Journal of Aircraft*, Vol. 17, April 1980, pp. 233-237.

[16]Kendall, E. R., "The Minimum Induced Drag, Longitudinal Trim and Static Longitudinal Stability of Two-Surface and Three-Surface Airplanes," AIAA Paper 84-2164, Aug. 1984.

[17]Rokhsaz, K. and Selberg, B. P., "Analytical Study of Three Surface Lifting Surfaces," to be presented at the SAE Business Aircraft Meeting, April 1985.

From the AIAA Progress in Astronautics and Aeronautics Series . . .

AERO-OPTICAL PHENOMENA—v. 80

Edited by Keith G. Gilbert and Leonard J. Otten, Air Force Weapons Laboratory

This volume is devoted to a systematic examination of the scientific and practical problems that can arise in adapting the new technology of laser beam transmission within the atmosphere to such uses as laser radar, laser beam communications, laser weaponry, and the developing fields of meteorological probing and laser energy transmission, among others. The articles in this book were prepared by specialists in universities, industry, and government laboratories, both military and civilian, and represent an up-to-date survey of the field.

The physical problems encountered in such seemingly straightforward applications of laser beam transmission have turned out to be unusually complex. A high intensity radiation beam traversing the atmosphere causes heat-up and breakdown of the air, changing its optical properties along the path, so that the process becomes a nonsteady interactive one. Should the path of the beam include atmospheric turbulence, the resulting nonsteady degradation obviously would affect its reception adversely. An airborne laser system unavoidably requires the beam to traverse a boundary layer or a wake, with complex consequences. These and other effects are examined theoretically and experimentally in this volume.

In each case, whereas the phenomenon of beam degradation constitutes a difficulty for the engineer, it presents the scientist with a novel experimental opportunity for meteorological or physical research and thus becomes a fruitful nuisance!

Published in 1982, 412 pp., 6×9, illus., $35.00 Mem., $55.00 List

TO ORDER WRITE: Publications Dept., AIAA, 1633 Broadway, New York, N.Y. 10019